EAST EUROPEAN JOURNAL OF PHYSICS. **2.** 179-187 (2025)
DOI:10.26565/2312-4334-2025-2-18 ISSN 2312-4334

THEORETICAL ANALYSIS OF INTERBAND SINGLE-PHOTON LIGHT ABSORPTION IN SEMICONDUCTORS: EFFECTS OF VALENCE-CONDUCTION BAND MIXING AND TEMPERATURE-DEPENDENT BANDGAP

Rustam Y. Rasulov[a], Voxob R. Rasulov[a]*, Nurillo U. Kodirov[a], Mardonbek Kh. Nasirov[c], Iqbol M. Eshboltaev[b]
[a] *Fergana State University, Fergana, Uzbekistan*
[b] *Kokand State pedagogical Institute, Kokand, Uzbekistan*
[c] *Fergana Polytechnic Institute, Fergana, Uzbekistan*
**Corresponding Author e-mail: vrrasulov83@gmail.com*
Received December 28, 2024; revised February 15, 2025; accepted February 20, 2025

This study presents a theoretical analysis of the spectral and temperature dependence of the single-photon absorption coefficient for linearly and circularly polarized light in semiconductors with diamond and zinc blende lattice structures. Optical transitions involving subbands of light and heavy holes and the conduction band are examined, incorporating effects such as temperature-dependent bandgap, valence-conduction band state mixing, and coherent saturation. The findings indicate that heavy holes contribute approximately 10 times more than light holes to single-photon absorption. Furthermore, the relationship between linear-circular dichroism and light intensity is explored, emphasizing the role of coherent saturation effects.
Keywords: *Semiconductor; Temperature dependence of the band gap; Mixing of valence band states with conduction band states; single-photon absorption; spectral-temperature dependence*
PACS: 71.20. – b, 71.28. + d

INTRODUCTION

Today, the development of not only micro-, but also nanoelectronics requires knowledge of the band structure of semiconductors, to which many literatures are devoted (for example, [1-5]).

A number of optical phenomena in both bulk and low-dimensional semiconductors are determined by the states of current carriers in several zones, the energies of which are close in comparison with the energy distances to other zones [5, 6]. For example, in *InSb* the conduction band (V-band) and valence band (c-band) are located quite close, and the spin-orbit splitting subband (SO-band) is relatively far away (Fig. 1*a*). In *GaAs*, the c- and V-bands are located close, and the upper-perturbed conduction band (c-band) is far away (Fig. 1*b*) [7].

However, most of them do not pay attention to the spin-orbit interaction of bands, taking into account the substitution of conduction band states to the states of the valence band.

In this regard, below we will consider the interband single-photon (quantum) absorption of polarized radiation in semiconductors with a diamond and zinc blende lattice, taking into account the substitution of conduction band states to the valence band states and the temperature dependence of the band gap [8,9].

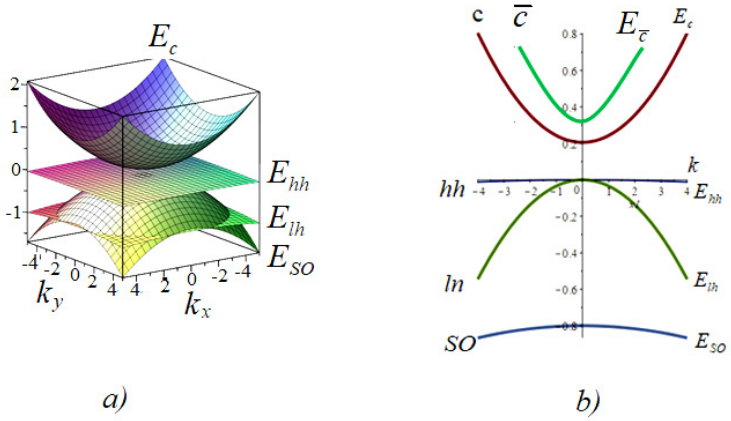

Figure 1. Multiband structure of indium antimonide: two (*a*) and multiband (*b*) approximation.

METHODS

The analysis is based on theoretical models that describe optical transitions in semiconductors with diamond and zinc blende lattice structures. The single-photon absorption coefficient was derived using the equilibrium distribution

Cite as: R.Y. Rasulov, V.R. Rasulov, N.U. Kodirov, M.Kh. Nasirov, I.M. Eshboltaev, East Eur. J. Phys. 2, 179 (2025), https://doi.org/10.26565/2312-4334-2025-2-18
© R.Y. Rasulov, V.R. Rasulov, N.U. Kodirov, M.Kh. Nasirov, I.M. Eshboltaev, 2025; CC BY 4.0 license

function of charge carriers and the composite matrix element of optical transitions. The bandgap energy E_g, was modeled using the Varshni and Passler formulas to account for temperature variations. Effective masses of electrons and holes were treated as temperature-dependent parameters to reflect their variations with thermal energy. The Hamiltonian was developed to include terms representing the mixing of light and heavy hole states with conduction band states, ensuring that spin-orbit coupling effects were incorporated for enhanced accuracy in narrow-gap semiconductors. Additionally, the impact of light intensity on absorption coefficients was evaluated through the Rabi parameter, to quantify coherent saturation effects.

All calculations were conducted using computational tools such as "Maple", with constants and material-specific parameters extracted from established databases and prior studies. This computational framework ensured consistency and reliability in deriving the temperature-dependent optical properties of the semiconductor materials under investigation.

INTERBAND AND INTRABAND MATRIX ELEMENTS OF THE MOMENTUM OPERATOR

Note that the probability of single-photon absorption (1PA) caused by the optical transition from state $|n,\vec{k}\rangle$ to state $|n',\vec{k'}\rangle$ is defined as [10-14]

$$W^{(1)}=\frac{2\pi}{\hbar}\left\langle\sum_{n,n',\vec{k}}\left|M^{(1)}_{n\vec{k},n'\vec{k}}\right|^2\right\rangle\left(f_{n\vec{k}}-f_{n'\vec{k}}\right)\delta\left(E_{n'}(\vec{k})-E_n(\vec{k})-\hbar\omega\right), \tag{1}$$

where $f_{n\vec{k}}\left(f_{n'\vec{k}}\right)$ is the equilibrium distribution function of current carriers in the initial (final) state, $M^{(1)}_{n\vec{k},n'\vec{k}}$ is the composite matrix element of a single-quantum optical transition, determined by the relation

$$M^{(1)}_{c,s;\,V,\Gamma_8,m}=\left(\frac{eA_0}{cm_0}\right)\vec{e}\cdot\vec{p}_{c,s;\,V,\Gamma_8,m}, \tag{2}$$

where $\vec{p}_{c,s;\,V,\Gamma_8,m}\frac{m_0}{\hbar}\frac{\partial}{\partial\vec{k}}\left[\widehat{\mathrm{H}}(\vec{k})_{c,s;\,V,\Gamma_8,m}\right]$ is the matrix element of the momentum operator, $A_0(\vec{e})$- is the amplitude value of the potential vector (polarization vector) of the light wave, $\widehat{\mathrm{H}}(\vec{k})$ is the Hamiltonian of current carriers in crystals with a zinc blende lattice, taking into account the admixture of light and heavy hole (Γ_8) subband states in the lower conduction band (Γ_6) (two-zone approximation) which takes the form [15]

$$H^{(\Gamma_8)}=E^0_{\Gamma_8}+\frac{\hbar^2k^2}{2m_0}-\frac{\hbar^2}{m_0^2}\frac{|p_{eV}|^2}{E_g}\begin{bmatrix}\frac{k_\perp^2}{2} & -\frac{k_zk_-}{\sqrt{3}} & -\frac{k^2}{\sqrt{12}} & 0\\ -\frac{k_zk_+}{\sqrt{3}} & \frac{2}{3}k_z^2+\frac{k_\perp^2}{6} & 0 & -\frac{k^2}{\sqrt{12}}\\ -\frac{k_+^2}{\sqrt{12}} & 0 & \frac{2}{3}k_z^2+\frac{k_\perp^2}{6} & \frac{k_zk_-}{\sqrt{3}}\\ 0 & -\frac{k_+^2}{\sqrt{12}} & \frac{k_zk_+}{\sqrt{3}} & \frac{k_\perp^2}{2}\end{bmatrix}, \tag{3}$$

where $p_{cV}=\langle S|p_z|Z\rangle, k_\pm=k_x\pm ik_y. E^0_{\Gamma_8}$- is the extreme value of the valence band, which we further consider to be the starting point for the energy of current carriers.

Note that if we take into account the spin-orbit splitting (Γ_7) of the valence band with distant bands, then in semiconductors with a zinc blende lattice, the symmetry allows them to have terms linear in the wave vector in the effective Hamiltonian (3), however, but, as a rule, such terms are neglected.

According to Hamiltonian (3), the matrix elements of the momentum operator for optical transitions between subbands of the valence band can be written in the form of the following matrix:

$$\left\|\vec{e}\cdot\vec{p}^{(\Gamma_8)}_{m',m}\right\|=\hbar k\begin{bmatrix}e'_z & +\zeta_g\frac{e'_-}{\sqrt{3}} & 0 & 0\\ +\zeta_g\frac{e'_+}{\sqrt{3}} & \left(1-\frac{4}{3}\zeta_g\right)e'_z & 0 & 0\\ 0 & 0 & \left(1-\frac{4}{3}\zeta_g\right)e'_z & -\frac{\zeta_ge'_-}{\sqrt{3}}\\ 0 & 0 & -\frac{\zeta_ge'_+}{\sqrt{3}} & e'_z\end{bmatrix}. \tag{4}$$

and for interband optical transitions

$$\left\|\vec{e}\cdot\vec{p}_{c,s;\,V,\Gamma_8,m}\right\|=p_{c,V}\begin{bmatrix}-\frac{e'_+}{\sqrt{2}} & e'_z\sqrt{\frac{2}{3}} & \frac{e'_-}{\sqrt{6}} & 0\\ 0 & -\frac{e'_+}{\sqrt{6}} & e'_z\sqrt{\frac{2}{3}} & \frac{e'_-}{\sqrt{2}}\end{bmatrix}, \tag{5}$$

Here $\zeta_g = \frac{|p_{c,V}|^2}{m_0 E_g}$ and it appears due to taking into account the admixture of the states of the valence band and the conduction band, $m', m = +3/2, +1/2, -1/2, -3/2$ eigenvalues of the angular momentum operator [5, 6], e'_x, e'_y, e'_z - $\vec{e}$ projections of the polarization vector relative to the coordinate system $x', y', z' \parallel \vec{k}$, $\vec{k}$- wave vector of current carriers, $p_{c,V}$ - Kane parameter and is determined in the following way

$$|p_{c,V}|^2 = \frac{3}{2} m_0 \frac{m_0 - m_c}{m_c} \frac{E_g(E_g + \Delta_{SO})}{2(E_g + \Delta_{SO}) + E_g}, \tag{6}$$

$E_g -$ band gap, Δ_{SO}-spin-orbit splitting width. Then: $\zeta_g = \frac{3m_0}{4} \frac{m_{hh} - m_{lh}}{m_{hh} m_{lh}}$ and the effective mass of electrons in the conduction band is expressed as

$$\frac{1}{m_c} = \frac{1}{m_0} + \frac{2}{3m_0^2} |p_{c,V}|^2 \left(\frac{2}{E_g} + \frac{1}{E_g + \Delta_{SO}} \right), \tag{7}$$

We write the temperature dependence of the band gap ($E_g(T)$) in the form of the Varshni formula [8]

$$E_g(T) = E_g(T = 0) - \gamma_T \frac{T^2}{T + T_V}, \tag{8}$$

and Passner formulas [9]

$$E_g(T) = E_g(T = 0) - \frac{\alpha \Theta_p}{2} \left[\left(1 + \left(\frac{2T}{\Theta_p} \right)^p \right)^{1/p} - 1 \right]. \tag{9}$$

Here γ_T, T_V, α, Θ_p, p- are constant quantities, the numerical values of which are given in [8, 9].

In particular, we choose the temperature dependences of the effective masses of electrons ($m_c(T)$) in the conduction band and holes ($m_{SO}(T)$) in the spin-orbit splitting subband as follows (see, for example, [8]):

$$\frac{m_0}{m_{SO}(T)} = \gamma_1 - \frac{E_P \Delta_{SO}}{3E_g(E_g + \Delta_{SO})}, \frac{m_0}{m_c(T)} = 1 + 2F + \frac{E_P(E_g + 2\Delta_{SO}/3)}{3E_g(E_g + \Delta_{SO})}. \tag{10}$$

Let us note here that with increasing temperature, $m_c(T)$ increases, and $m_{SO}(T)$ decreases, and this case has a noticeable effect, as shown below, on the frequency and temperature dependences of the light absorption coefficient.

From (4) and (5) it is clear that the composite matrix element depends on the type of single-photon optical transitions. In particular, for an optical transition from the heavy hole subband to the conduction band is determined by the relation

$$M^{(1)}_{c,\pm 1/2; hh, \pm 3/2} = \frac{1}{\sqrt{2}} \left(\frac{eA_0}{c\hbar} \right) p_{c,V} \begin{bmatrix} -e'_- & 0 \\ 0 & e'_+ \end{bmatrix}; \tag{11}$$

from the subband of light holes to the conduction band:

$$M^{(1)}_{c,\pm 1/2; lh, \pm 1/2} = \frac{1}{\sqrt{6}} \left(\frac{eA_0}{c\hbar} \right) p^*_{c,V} \begin{bmatrix} 2e'_z & -e'_- \\ e'_+ & 2e'_z \end{bmatrix}; \tag{12}$$

from the subzone of heavy holes to the subzone of heavy holes:

$$M^{(1)}_{hh, \pm 3/2; hh, \pm 3/2} = \left(\frac{eA_0}{c\hbar} \right) \hbar k e'_z \begin{bmatrix} 1 & 0 \\ 0 & 1 \end{bmatrix}, \tag{13}$$

from the subzone of light holes to the subzone of light holes:

$$M^{(1)}_{lh, \pm 1/2; lh, \pm 1/2} = \frac{1}{3} \left(\frac{eA_0}{c\hbar} \right) \hbar k (3 - 4\zeta_g) e'_z \begin{bmatrix} 1 & 0 \\ 0 & 1 \end{bmatrix}; \tag{14}$$

from the subzone of heavy holes to the subzone of light holes:

$$M^{(1)}_{lh, \pm 1/2; hh, \pm 3/2} = \frac{\zeta_g}{\sqrt{3}} \left(\frac{eA_0}{c\hbar} \right) \hbar k \begin{bmatrix} e'_- & 0 \\ 0 & -e'_+ \end{bmatrix}. \tag{15}$$

Spectral dependence means that the interband absorption coefficient takes different values as the frequency of light (or photon energy) changes. The effect of temperature is mainly manifested through the following factors: Change in the energy gap between bands: As temperature increases, the bandgap of semiconductors narrows, which affects the absorption spectrum. Effect of phonons: With increasing temperature, the number of phonons (thermal vibrations) in the

crystal lattice increases, which influences the movement of electrons and holes. Optical absorption width: As temperature rises, the absorption spectrum may expand, or the absorption rate may decrease.

Coherent saturation is a phenomenon in which interband absorption decreases under the influence of intense light fields. In other words, under strong laser radiation or other optical excitations, the frequency and intensity of quantum transitions change in such a way that absorption decreases. This effect is of great importance in quantum mechanics and laser physics.

This concept describes the temporal variations of light absorption processes in semiconductors. The absorption rate and duration depend on the power of the light source, modulation frequency, and the physical properties of the material.

Note that the coefficient of single-quantum light absorption is determined by the expression (see, for example, [12])

$$K^{(1)} = \frac{2\pi}{\hbar}\frac{\hbar\omega}{I}\sum_{\vec{k},L,m;L\prime,m\prime}\left(f^{(1)}_{L\prime,\vec{k}} - f^{(1)}_{L,\vec{k}}\right)\left|M^{(1)}_{L,m;\,L\prime,m\prime}(\vec{k})\right|^2\delta\left(E_{L\prime,\vec{k}} - E_{L,\vec{k}} - \hbar\omega\right). \tag{16}$$

Here $L,m(L',m') = lh,m' = \pm 1/2(hh,m' = \pm 3/2)$- for heavy (light) holes), where their energy spectrum has the form $E_{L,\vec{k}} = -\hbar^2k^2/(2m_L)$, $L,m(L',m') = \mathrm{c},m' = \pm 1/2$- for electrons in the conduction band, whose energy spectrum is: $E_{c,\vec{k}} = E_g + \hbar^2k^2/(2m_c)$. Then, taking into account relations (2)-(5) the light absorption coefficient:

a) for optical transitions from the heavy hole subband to the conduction band will be written as

$$K^{(1)}_{\mathrm{c},\pm 1/2;hh,\pm 3/2} = \frac{4\pi^2e^2}{3\hbar n_\omega c}\left|p_{c,V}\right|^2\frac{\mu_+^{(c,hh)}}{\hbar^2}\frac{k^{(\omega)}_{\mathrm{c},lh}}{\hbar\omega}\left\langle\frac{|e\prime_\pm|^2}{\sqrt{1+\zeta_{hh}|e\prime_\pm|^2}}\right\rangle\cdot\left[f_c\left(k^{(\omega)}_{\mathrm{c},hh}\right) - f_{hh}\left(k^{(\omega)}_{\mathrm{c},hh}\right)\right], \tag{17}$$

b) for optical transitions from the subband of light holes to the conduction band we have

$$K^{(1)}_{\mathrm{c},\pm 1/2;lh,\pm 1/2} = \frac{4\pi^2e^2}{3\hbar n_\omega c}\left|p_{c,V}\right|^2\frac{\mu_+^{(c,lh)}}{\hbar^2}\frac{k^{(\omega)}_{\mathrm{c},lh}}{\hbar\omega}\left\langle\frac{4e\prime_z{}^2+e\prime_\perp{}^2}{\sqrt{1+\zeta_{lh}(4e\prime_z{}^2+e\prime_\perp{}^2)}}\right\rangle\cdot\left[f_c\left(k^{(\omega)}_{\mathrm{c},lh}\right) - f_{hh}\left(k^{(\omega)}_{\mathrm{c},lh}\right)\right], \tag{18}$$

Here it is taken into account that $\left(\frac{\mathrm{eA_0}}{\mathrm{c}\hbar}\right)^2 = \frac{2\pi\mathrm{e}^2}{\mathrm{n_\omega c}}\frac{\mathrm{I}}{(\hbar\omega)^2}$, $\zeta_{\mathrm{hh}} = 4\frac{\alpha_\omega}{\hbar^2\omega^2}\left(\frac{\mathrm{eA_0}}{\mathrm{c}\hbar}\right)^2\left|\mathrm{p_{c,V}}\right|^2$, $\zeta_{\mathrm{lh}} = \zeta_{\mathrm{hh}}/3$,$\alpha_\omega = 6\omega^2\mathrm{T}^{(1)}_{\mathrm{hh}}\mathrm{T}^{(1)}_{\mathrm{lh}}\frac{\mathrm{I}}{\mathrm{I_0}}$, $I_0 = \frac{cn_\omega\hbar^3\omega^3}{2\pi|B|}$, $k^{(\omega)}_{\mathrm{c},L} = \sqrt{\frac{2\mu_+^{(c,L)}}{\hbar^2}\left(\hbar\omega - E_g\right)}$, $\mu_+^{(c,L)} = \frac{m_cm_L}{m_c+m_L}(L = lh,\ hh)$. $f_c\left(k^{(\omega)}_{\mathrm{c},lh},T\right)$, $f_{hh}\left(k^{(\omega)}_{\mathrm{c},lh},T\right)$ and $f_{hh}\left(k^{(\omega)}_{\mathrm{c},lh},T\right)$- distribution functions of electrons, light and heavy holes participating in optical transitions from subbands of the valence band to the conduction band; symbol $\langle\ldots\rangle$ denotes averaging over solid angles of the wave vector.

Carrying out angular averaging over the solid angles of the wave vector of current carriers in (18, 19), we obtain that both the 1FP coefficient $\mathrm{K}^{(1)}_{\mathrm{c},\pm 1/2;\mathrm{hh},\pm 3/2}(\mathrm{I})$ (Fig. 2 *a*) and the linear-circular dichroism coefficient $\eta^{(1)}_{\mathrm{c},\pm 1/2;\mathrm{hh},\pm 3/2}(\mathrm{I}) = \frac{\mathrm{W}^{(1,\mathrm{circ})}_{\mathrm{c},\pm 1/2;\mathrm{hh},\pm 3/2}(\mathrm{I})}{\mathrm{W}^{(1,\mathrm{linear})}_{\mathrm{c},\pm 1/2;\mathrm{hh},\pm 3/2}(\mathrm{I})}$ (Fig. 2 *b*) decrease with increasing Rabi parameter $\zeta_{\mathrm{hh}}(I)$ (light intensity) for optical transitions from the heavy hole subband to the conduction band in *InAs*. Calculations show that in *InSb* the light absorption coefficient $\mathrm{K}^{(1)}_{\mathrm{c},\pm 1/2;\mathrm{hh},\pm 3/2}(\zeta_{\mathrm{hh}} = 0)$ is approximately 5 times less than the light absorption coefficient due to optical transitions from the light hole subband to the conduction band, and the coefficient $\eta^{(1)}_{\mathrm{c},\pm 1/2;\mathrm{hh},\pm 3/2}(\mathrm{I}) = \frac{\mathrm{W}^{(1,\mathrm{circ})}_{\mathrm{c},\pm 1/2;\mathrm{hh},\pm 3/2}(\mathrm{I})}{\mathrm{W}^{(1,\mathrm{linear})}_{\mathrm{c},\pm 1/2;\mathrm{hh},\pm 3/2}(\mathrm{I})}$ decreases by approximately 1.1 times.

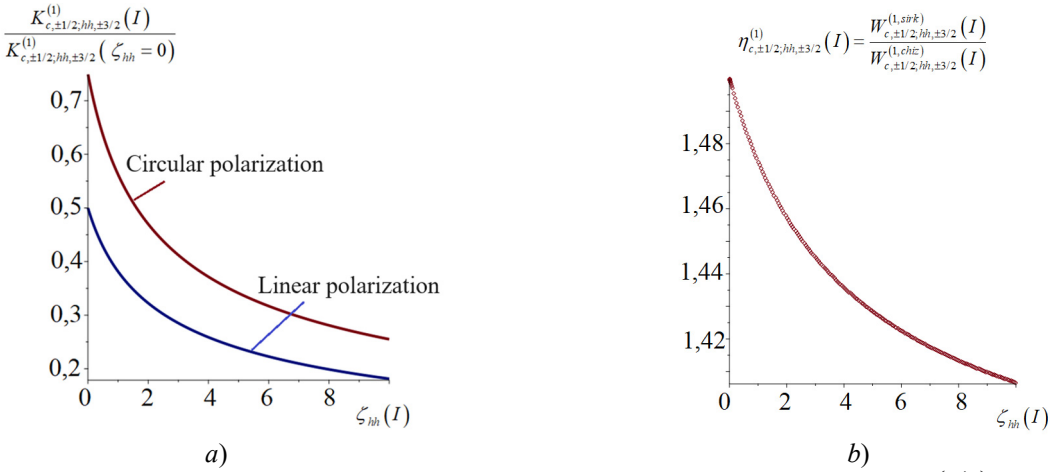

Figure 2. Dependence of the coefficients 1FA $K^{(1)}$ (*a*) and linear-circular dichroism $\eta^{(1)}_{\mathrm{c},\pm 1/2;hh,\pm 3/2}(I) = \frac{W^{(1,circ)}_{\mathrm{c},\pm 1/2;hh,\pm 3/2}(I)}{W^{(1,linear)}_{\mathrm{c},\pm 1/2;hh,\pm 3/2}(I)}$ (b) on the Rabi parameter $\zeta_{hh}(I)$ (on light intensity) for optical transitions from the heavy hole subband to the conduction band in InAs.

Thus, it was shown that the main contribution to the single quantum absorption coefficient of light comes from light holes participating in interband optical transitions from the subbands of the valence band to the conduction band.

Next, it is advisable to analyze the spectral-temperature dependences of the distribution functions of heavy ($f_{hh}(\omega,T)$) and light ($f_{lh}(\omega,T)$) holes (see Fig. 3), since $K^{(1)}(\omega,T)$ is determined by the spectral-temperature dependence $f_{hh}(\omega,T)$ and $f_{lh}(\omega,T)$ (see formula (18), (19). Calculations using spectral temperature dependences $f_{hh}(\omega,T)$ and $f_{lh}(\omega,T)$ (in the approximation of non-degenerate statistics [16] show that for *InSb*:

a) at a fixed frequency, with increasing temperature, the distribution functions increase, reach a maximum, and then decrease, since the distribution functions consist of the product of $T^{-3/2}$ and $\exp(-E^*/k_B T)$, where E^*-is the energy of photoexcited holes;

b) the maximum values of the distribution functions decrease with increasing frequency, the relative change of which depends on the band parameters of the crystal, for example, on $E_g(T)$. In particular, in narrow-gap crystals this value is greater than in wide-gap crystals: for example, in *InSb* it is approximately 5.4 times greater than in *InSb*;

c) if we take into account the dependence of band parameters on temperature (according to (8) and (9)), then the distribution function of light (heavy) holes in *InSb* decreases by approximately 5.3 (2.5) times, and in *InAs* - by 5,2 (2) times.

The above cases certainly influence the spectral-temperature dependences $K^{(1)}(\omega,T)$, which are analyzed below.

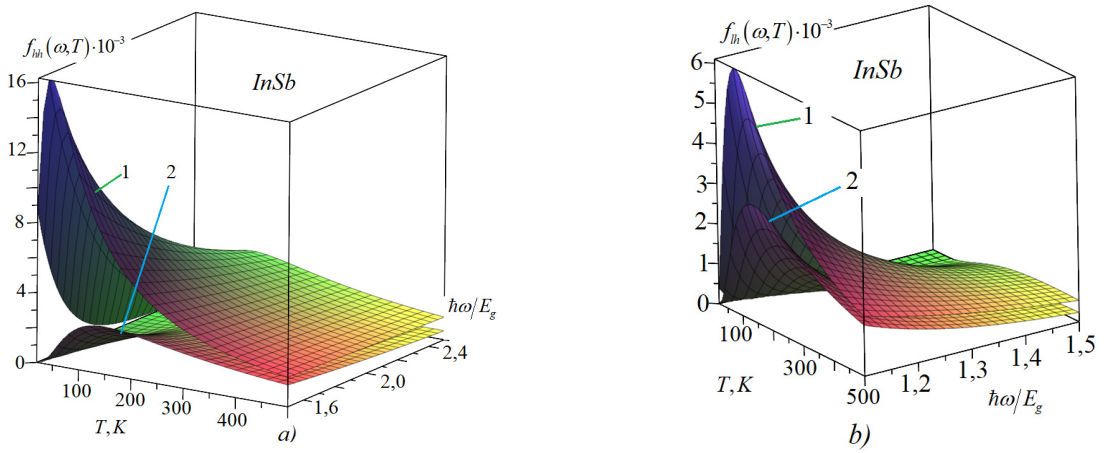

Figure 3. Spectral-temperature dependences of the distribution functions of heavy (*a*) and light (*b*) holes in *InSb*. 1 (2) – corresponds to $E_g = E_g(T = 0\ K)(E_g(T))$

In Figure 4 shows spectral-temperature dependences $K^{(1)}(\omega,T)$ for optical transitions of subbands of light and heavy holes into the conduction band in InSb when illuminated with light of linear (1) and circular (2) polarization, where the temperature dependence of band parameters is not taken into account and the maximum value of coefficient $K^{(1,linear)}_{c,\pm1/2;hh,\pm3/2}(\omega,T)$ was taken as one unit , and the Rabi coefficient was chosen to be 0.5 [17, 18].

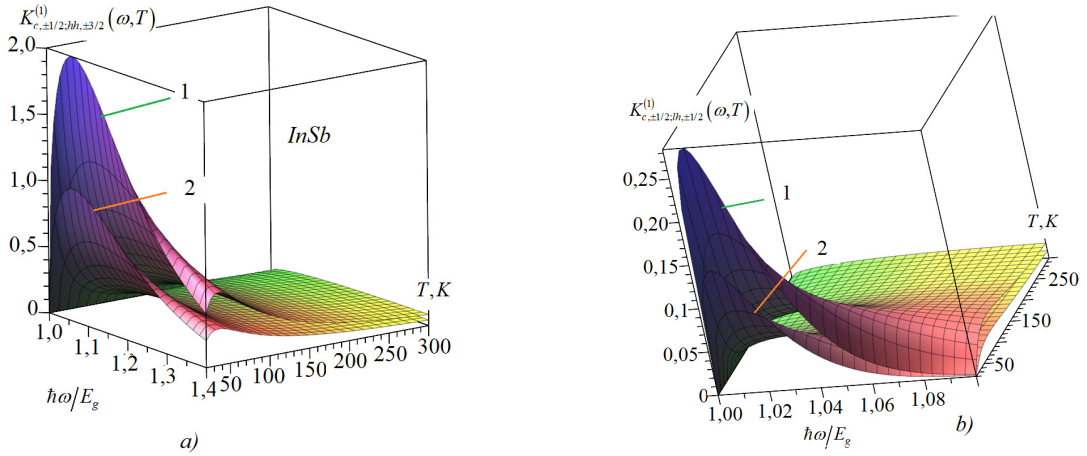

Figure 4. Spectral-temperature dependences of the 1FA coefficient of polarized light due to optical transitions from the subband of heavy $K^{(1)}_{c,\pm1/2;hh,\pm3/2}(\omega,T)$ (a) and light $K^{(1)}_{c,\pm1/2;lh,\pm1/2}(\omega,T)$ (b) holes to the conduction band of InSb (a), where 1 (2) corresponds to light of circular (linear) polarization. The calculations did not take into account the temperature dependence $E_g(T)$ and the maximum value of coefficient $K^{(1,linear)}_{c,\pm1/2;hh,\pm3/2}(\omega,T)$ was taken as one unit, and the Rabi coefficient was chosen equal to 0.5.

In this case, with increasing frequency and temperature, $K^{(1)}(\omega,T)$ increases (as do the hole distribution functions), reaches a maximum, and then decreases. In Figure 5 shows graphs of values $K^{(1,)}_{c,\pm1/2;hh,\pm3/2}(\omega,T)$ and $K^{(1,)}_{c,\pm1/2;lh,\pm1/2}(\omega,T)$ calculated taking into account the temperature dependence $E_g(T)$. Calculations show that the amplitude value of the 1FP coefficient in the region of low frequencies and temperatures sharply decreases with increasing temperature. This situation is explained by the temperature and spectral dependences of the hole distribution functions. We also note that the transition of value $K^{(1,)}_{c,\pm1/2;hh,\pm3/2}(\omega,T)$ through a maximum in the temperature dependence is observed in the frequency range ω≅$1{,}2E_g/\hbar$ for *InSb*, ω≅$1{,}1E_g/\hbar$ for *InAs* and ω≅$1{,}005E_g/\hbar$ 110 K GaAs for both linear and circular polarization, and the temperature corresponding to this maximum is higher, the higher bandgap width. In particular, this temperature is 45 K for *InSb* at $\omega = 1{,}3E_g/\hbar$, 80 K for *InAs* at $\omega = 1{,}4E_g/\hbar$ and 110 K for GaAs at $\omega = 1{,}02E_g/\hbar$.

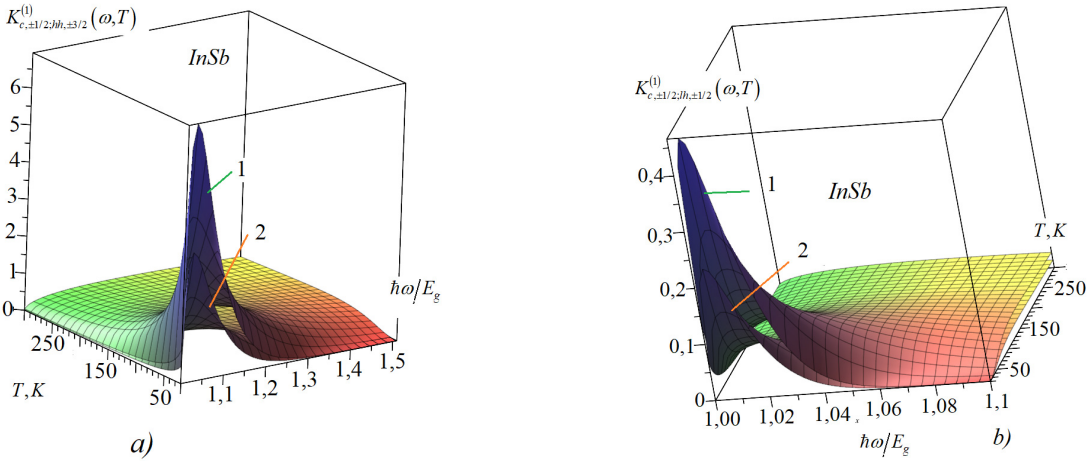

Figure 5. Spectral-temperature dependences of the 1PA coefficient caused by optical transitions from the subband of heavy holes $K^{(1)}_{c,\pm1/2;hh,\pm3/2}(\omega,T)$ (*a*) and light holes $K^{(1)}_{c,\pm1/2;lh,\pm1/2}(\omega,T)$ (*b*) to the conduction band in *InSb*), where 1 (2) corresponds to light of circular (linear) polarization. The calculations took into account the temperature dependence E_g (T) and the maximum value of coefficient $K^{(1,linear)}_{c,\pm1/2;hh,\pm3/2}(\omega,T)$ was taken as one unit, and the Rabi coefficient was chosen equal to 0.5.

In Figure 6 shows the spectral-temperature dependences of the ratios $\tilde{K}^{(1)}_{c,\pm1/2;lh,\pm1/2}/K^{(1)}_{c,\pm1/2;lh,\pm1/2}$ and in *InSb* crystals. Here $\tilde{K}^{(1)}_{c,\pm1/2;lh,\pm1/2}$ and $K^{(1)}_{c,\pm1/2;lh,\pm1/2}$ the coefficients 1FP taking into account (Fig. 5 a) and without taking into account (Fig. 5 *b*) the temperature dependence of the band parameters, where the contribution of the coherent saturation effect is neglected (therefore $K^{(1)}_{c,\pm1/2;hh,\pm3/2}$ do not depend on the degree of polarization of light). From this figure it is clear that the contribution of optical transitions from the heavy hole subband is greater than the contribution of optical transitions from the light hole subband to the conduction band in InSb, and this contribution increases when taking into account $E_g(T)$.

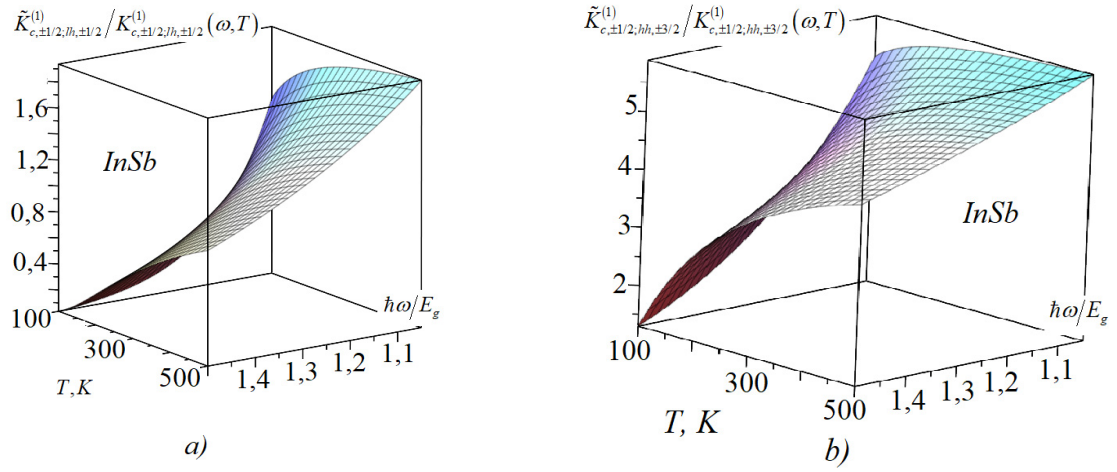

Figure 6. Spectral-temperature dependence of the ratio $\tilde{K}^{(1)}_{c,\pm1/2;lh,\pm1/2}/K^{(1)}_{c,\pm1/2;lh,\pm1/2}$ in *InSb*, where $\tilde{K}^{(1)}_{c,\pm1/2;lh,\pm1/2}$ $\left(K^{(1)}_{c,\pm1/2;lh,\pm1/2}\right)$ is the coefficient 1PA taking into account (*a*) and without taking into account (*b*) the temperature dependence of band parameters, where the contribution of the coherent saturation effect is neglected.

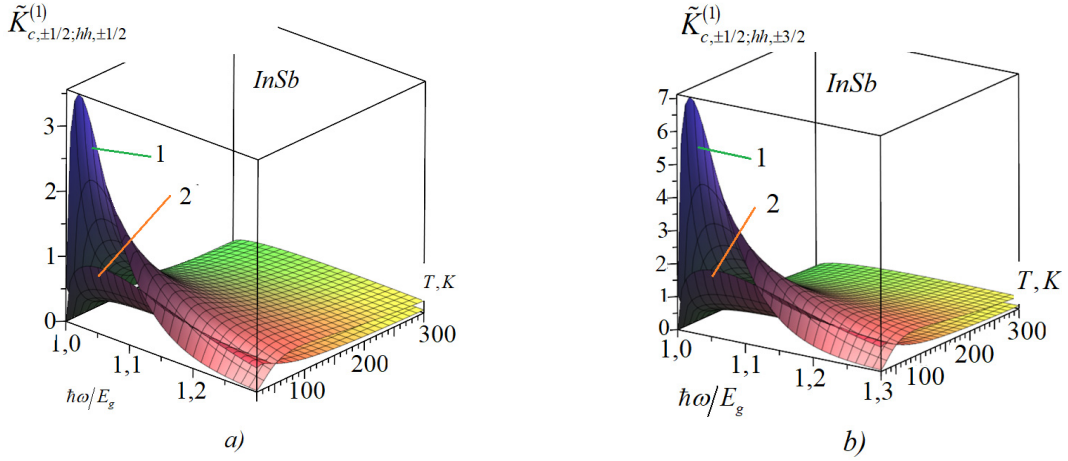

Figure 7. Spectral-temperature dependence of the ratio $\tilde{K}^{(1)}_{c,\pm1/2;lh,\pm1/2}/K^{(1)}_{c,\pm1/2;lh,\pm1/2}$ for light of linear (line 1) and circular (line 2) polarization, caused by optical transitions from the subband of light (*a*) and heavy (*b*) holes to the conduction band of *InSb*. In the calculations, the maximum value of the coefficient $K^{(1,linear)}_{c,\pm1/2;hh,\pm3/2}(\omega,T)$ was taken as one, and the Rabi coefficient was chosen equal to 0.5.

In Figure 7 shows the spectral-temperature dependences of the ratio $\tilde{K}^{(1)}_{c,\pm1/2;lh,\pm1/2}/K^{(1)}_{c,\pm1/2;lh,\pm1/2}$ for linearly (line 1) and circularly polarized light (line 2), caused by interband optical transitions from the light hole subband to the InSb conduction band, from where, that $\tilde{K}^{(1)}_{c,\pm1/2;lh,\pm1/2}/K^{(1)}_{c,\pm1/2;lh,\pm1/2}$ in a narrow-gap semiconductor for linear polarization in low-temperature regions is significantly greater than for circular polarization when taking into account the effect of coherent saturation. In this case, as calculations show, in the low-temperature region, the main contribution comes from optical transitions from the heavy hole subband, regardless of the degree of light polarization, both with and without taking into account the contribution of the coherent saturation effect.

According to (17), the spectral-temperature dependences $K^{(1)}(\omega,T)$ are determined by the distribution functions of heavy and light holes.

Consequently, taking into account relations (8) and (9) allows us to compare distribution functions both by temperature (at a fixed frequency) and by frequency (at a fixed temperature).

In Figure 8 shows the spectral-temperature dependence of the hole distribution functions $f(\omega,T)$, calculated taking into account the temperature dependence of the band gap and effective masses in *InSb*, where graphs 1(2) and 3(4) correspond to light (heavy) holes, calculated from (8) and (9).

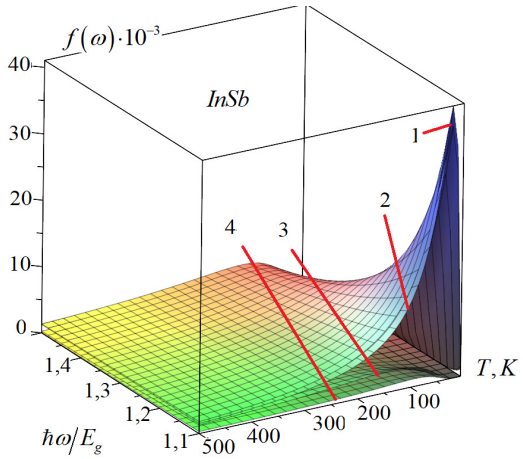

Figure 8. Spectral - temperature dependence of the hole distribution functions, calculated taking into account the temperature dependence of the band gap and effective masses in *InSb*, where graphs 1 (2) and 3 (4) correspond to light (heavy) holes, calculated from (8) and (9).

From these graphs it can be seen that in the region of low frequencies and high temperatures $f(\omega,T)$ decreases slightly (less than 5%) when moving from (8) to (9): the amplitude value of the distribution functions of heavy holes decreases by approximately 1.7 times in the low-frequency range. However, in the region of high frequencies and low temperatures the opposite is true.

Note that since the coefficient of single-photon interband absorption of light is proportional to the wave vector of photoexcited current carriers $k^{(\omega)}_{c,L}=\left[2m_cm_L\hbar^{-2}\left(\hbar\omega-E_g\right)/(m_c+m_L)\right]^{1/2}$, then under condition $\hbar\omega=E_g$ it becomes

zero, which means that light absorption satisfies condition $\hbar\omega \geq E_g$, where $E_g = E_g(T=0)$. But if we take into account expressions (8) and (9), then $k_{c,L}^{(\omega)}(T) = \left\{2m_c(T)m_L\hbar^{-2}\left(\hbar\omega - E_g(T)\right)/[m_c(T)+m_L]\right\}^{1/2}$ increases with increasing temperature, since with increasing temperature $E_g(T)$ decreases. As a result, the light absorption edge satisfies condition $\hbar\omega \leq E_g(T=0)$ (instead of $\hbar\omega \geq E_g$).

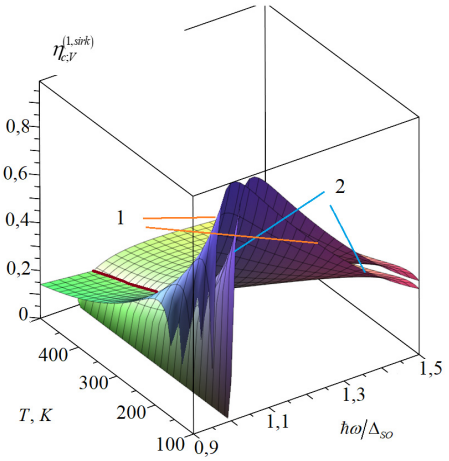

Figure 9. Spectral-temperature dependence of the relative total 1PA $\eta_{c;V}^{(1,circ)} = \left(\widetilde{K}_{c,\pm1/2;hh,\pm1/2}^{(1,circ)} + \widetilde{K}_{c,\pm1/2;hh,\pm3/2}^{(1,circ)}\right)/\left(K_{c,\pm1/2;hh,\pm3/2}^{(1,circ)} + K_{c,\pm1/2;hh,\pm3/2}^{(1,circ)}\right)$ for circularly polarized light in *InSb*. In the calculations, the maximum value of the coefficient $\widetilde{K}_{c,\pm1/2;lh,\pm1/2}^{(1,linear)}$ was taken as one, and the Rabi coefficient was chosen equal to 0.5, where graphs 1 and 2 were calculated using formulas (8) and (9), respectively.

Calculations show that at room temperature the contribution of heavy holes to coefficient $\widetilde{K}_{c,m;L,m'}^{(1)}(\omega,T)$ is approximately 10 times greater than the contribution of light holes in the frequency range satisfying condition $1.1E_g < \hbar\omega < 1.5E_g$. This situation also occurs in the spectral-temperature dependences of the resulting 1PA coefficient (see Fig. 9), and the physical nature of these dependences is explained by a similar frequency dependence of the nonequilibrium distribution functions of current carriers.

CONCLUSIONS

In conclusion, this study provides an in-depth theoretical framework to understand the mechanisms underlying single-photon interband absorption in semiconductors with diamond and zinc blende lattice structures. By incorporating temperature-dependent bandgap variations and the mixing of valence and conduction band states, the research highlights key factors that influence the absorption process. Heavy hole contributions were found to dominate over light hole contributions, with a significant enhancement of absorption coefficients in narrow-gap semiconductors at lower temperatures. The findings also reveal a pronounced dependence of linear-circular dichroism on light intensity, attributed to the coherent saturation effects.

The results underscore the critical role of temperature and band structure in determining optical absorption properties, offering valuable insights for applications in optoelectronic devices. However, the study also emphasizes the need for experimental validation to verify these theoretical predictions. Future work should focus on extending the analysis to a broader class of semiconductors and exploring the interplay of higher-order effects, such as spin-orbit coupling, to refine the understanding of optical absorption phenomena. These advancements will not only enhance the theoretical accuracy but also pave the way for practical implementations in advanced semiconductor technologies.

ORCID

Rustam Y. Rasulov, https://orcid.org/0000-0002-5512-0654; **Voxob R. Rasulov,** https://orcid.org/0000-0001-5255-5612

REFERENCES

[1] I.M. Tsidilkovski, *Band Structure of Semiconductors: International Series on the Science of the Solid State*, (Pergamon Press, 2016).
[2] G.L. Bir, and G.E. Pikus, *Symmetry and Strain-induced Effects in Semiconductors*, (I.P.S.T., 1975).
[3] E.L. Ivchenko, and R.Ya. Rasulov, *Symmetry and real band structure of semiconductors*, (FAN, Tashkent, 1992). (in Russian)
[4] G.G. Zegrya, and V.I. Perel, *Fundamentals of semiconductor physics*, (Fizmatlit, 2009). (in Russian)
[5] G. Pikus, and E.L. Ivchenko, *Superlattices and Other Heterostructures: Symmetry and Optical Phenomena, Springer Series in Solid-State Sciences*, Vol. 110, (Springer Verlag, 2nd edition, 1997).
[6] E.L. Ivchenko, *Optical Spectroscopy of Semiconductor Nanostructures*, Vol. XII, (Alpha Science International Ltd., Harrow, UK, 2005).
[7] M.M. Glazov, *Physics of low-dimensional systems. Course lecture*, (2022). (in Russian)

[8] I. Vurgaftman, J.R. Meyer, and L.R. Ram-Mohan, "Band parameters for III–V compound semiconductors and their alloys," Journal of Applied Physics, **89**, 5815–5875 (2001). https://doi.org/10.1063/1.1368156
[9] R. Päßler, "Parameter Sets Due to Fittings of the Temperature Dependencies of Fundamental Bandgaps in Semiconductors," Phys. Stat. Sol. (b), **216**, 975-1007 (1999). https://doi.org/10.1002/(SICI)1521-3951(199912)216:2<3.CO;2-E
[10] E.L. Ivchenko, "Two-photon absorption of light and optical orientation of free carriers," Physics, 14(12), 3489-3496 (1972). (in Russian)
[11] R.Ya. Rasulov, "Linear-circular dichroism in multiphoton intersubband absorption in semiconductors," Phys. **35**(6), 1674-1678 (1993). https://journals.ioffe.ru/articles/viewPDF/14966
[12] R.Ya. Rasulov, V.R. Rasulov, M.Kh. Kuchkarov, and I.M. Eshboltaev, "Interband multiphoton absorption of polarized radiation and its linear circular dichroism in semiconductors in the kane approximation." Russian Physics Journal, **65**(10), 1746-1754 (2023). https://doi.org/10.1007/s11182-023-02825-3
[13] R.Ya. Rasulov, V.R. Rasulov, and I.M. Eshboltaev, "Linearly and circular dichroism in a semiconductor with a complex valence band with allowance for four-photon absorption of light," Phys. Solid State, **59**, 463–468 (2017). https://doi.org/10.1134/S1063783417030283
[14] V.R. Rasulov, R.Ya. Rasulov, N.U. Kodirov, and U.M. Isomaddinova, "Interband single-photon absorption and its linear-circular dichroism in crystals taking into account the effect of coherent saturation," Physics of the Solid State, **65**(7), 1224-1230 (2023). https://journals.ioffe.ru/articles/viewPDF/56410
[15] E.L. Ivchenko, Physics of low-dimensional systems, 2015. https://solid.phys.spbu.ru/images/Ivch_lec15.pdf (in Russian)
[16] Y.U. Peter, and M. Cardona, Fundamentals of Semiconductors: Physics and Materials Properties, (Springer, 2010).
[17] N.V. Leppenen, E.L. Ivchenko, and L.E. Golub, "Nonlinear optical absorption and photocurrents in topological insulators," Phys. Rev. B, **105**, 115306 (2022). https://doi.org/10.1103/PhysRevB.105.115306
[18] D.A. Parshin, and A.R. Shabaev, "Theory of linear IR absorption by semiconductors with degenerate bands," Zh. Exp. Teor. Fiz. **92**(4), 1471-1484 (1987). http://jetp.ras.ru/cgi-bin/dn/e_065_04_0827.pdf (in Russian)

ТЕОРЕТИЧНИЙ АНАЛІЗ МІЖЗОННОГО ОДНОФОТОННОГО ПОГЛИНАННЯ СВІТЛА В НАПІВПРОВІДНИКАХ: ЕФЕКТИ ЗМІШУВАННЯ ЗОН ВАЛЕНТНОЇ ПРОВІДНОСТІ ТА ТЕМПЕРАТУРНО-ЗАЛЕЖНОЇ ЗАБОРОНЕНОЇ ЗОНИ

Рустам Я. Расулов[a], Вохоб Р. Расулов[a], Нурілло У. Кодіров[a], Мардон Х. Насіров[c], Ікбол М. Ешболтаєв[b]
[a]Ферганський державний університет, Фергана, Узбекистан
[b]Кокандський державний педагогічний інститут, Коканд, Узбекистан
[c]Ферганский политехнический институт, Фергана, Узбекистан

У цьому дослідженні представлено теоретичний аналіз спектральної та температурної залежності коефіцієнта однофотонного поглинання лінійно та циркулярно поляризованого світла в напівпровідниках із ґратковими структурами алмазу та цинкової обманки. Розглядаються оптичні переходи, що включають підзони легких і важких дірок і зону провідності, включаючи такі ефекти, як температурно-залежна заборонена зона, змішування станів валентної зони провідності та когерентне насичення. Отримані дані показують, що важкі діри сприяють однофотонному поглинанню приблизно в 10 разів більше, ніж легкі. Крім того, досліджується зв'язок між лінійно-круговим дихроїзмом та інтенсивністю світла, підкреслюючи роль когерентних ефектів насичення.

Ключові слова: *напівпровідник; температурна залежність забороненої зони; змішування станів валентної зони зі станами зони провідності; однофотонне поглинання; спектрально-температурна залежність*